IEEE Access
Multidisciplinary ⋮ Rapid Review ⋮ Open Access Journal

Received February 9, 2021, accepted February 24, 2021, date of publication March 1, 2021, date of current version March 9, 2021.

Digital Object Identifier 10.1109/ACCESS.2021.3062797

Adaptive LADRC Parameter Optimization in Magnetic Levitation

QINGHUA OUYANG, (Graduate Student Member, IEEE), KUANGANG FAN, (Member, IEEE), YAHUI LIU, (Student Member, IEEE), AND NA LI, (Student Member, IEEE)

School of Electrical Engineering and Automation, Jiangxi University of Science and Technology, Ganzhou 341000, China
Magnetic Suspension Technology Key Laboratory of Jiangxi Province, Jiangxi University of Science and Technology, Ganzhou 341000, China

Corresponding author: Kuangang Fan (kuangangfriend@163.com)

This work was supported in part by the National Natural Science Foundation of China under Grant 61763018, in part by the 03 Special Project and 5G Program of Science and Technology Department of Jiangxi Province under Grant 20193ABC03A058, in part by the Key Foundation of Education Committee of Jiangxi Province under Grant GJJ170493 and Grant GJJ190451, and in part by the Program of Qingjiang Excellent Young Talents of the Jiangxi University of Science and Technology.

ABSTRACT In this study, an adaptive linear active disturbance rejection control is proposed to achieve steady levitation of the magnetic levitation ball. The proposed algorithm was designed and its convergence was proven via derivation. It can address the difficulty in parameter tuning of the controller and realize the real-time self-adaptive optimization of parameters. Besides, to verify the effectiveness of the proposed parameter tuning strategy, we analysed the anti-interference ability and tracking effects of SMC, LADRC and A-LADRC in different cases. Finally, the results showed that the anti-interference ability of A-LADRC is stronger than SMC and LADRC. In addition, the anti-interference effect intensifies when the interference increases. The designed controller also performs the best tracking performance among these three controllers. Therefore, A-LADRC exhibits better robustness and dynamic performance.

INDEX TERMS Magnetic levitation, A-LADRC, SMC, anti-interference ability.

I. INTRODUCTION

Since the magnetic levitation technology [1] does not directly contact the mechanical equipment, there is no need to lubricate the equipment, which extends its life. And it has been widely used in aerospace, transportation and industry [2]–[4]. With the significantly improvement in the manufacturing process of permanent magnet materials, hybrid levitation has become a hot spot in new magnetic levitation technology [5], [6] once again. Compared with pure electromagnetic levitation, hybrid levitation increases the difficulty of levitation control. It is susceptible to magnetic materials, external interference and changes in its own parameters [7], [8]. Sun *et al.* [9] has presented a neural network-based supervisor control approach to realize effective control for the scenarios of random disturbance force, flexible track, and time-delay of maglev vehicle systems. Therefore, how to realize its stable suspension control has became the main topic of researchers [10]–[12].

Most of the controlled plants are complex in structure and the models are difficult to obtain, thus tuning of the controller parameters without a detailed model is critical in practice. Han *et al.* [13], [14] introduced active disturbance rejection control (ADRC) theory in 1998.The ADRC inherited the advantages of the classic PID by reducing the total disturbance of various uncertain factors. Accordingly, the controlled object demonstrated satisfactory adaptability and robustness [15]. Gao *et al.* [16] applied the concept of frequency scale to linearize ADRC and proposed an easy-to-implement linear ARDC (LADRC), which solved the problems [17], [18] of the early ADRC tuning by linking the parameters in the controller with the bandwidth. Hence, LADRC has been widely used in various fields. However, he did not study the influence of b_0 on the controller. In order to solve the problem of parameter optimization and setting in active disturbance rejection control. Chen *et al.* [19] put forward an improved LADRC parameter-tuning method. It can determined parameters of the controller under the premise of knowing the adjustment time. However, the appropriate adjustment time must first be determined to obtain the bandwidth parameter. Yuan *et al.* [20] started from the frequency domain and proposed a method of frequency band characteristic curve. It can solve the difficulty of parameter tuning in linear active disturbance rejection control (LADRC).

The associate editor coordinating the review of this manuscript and approving it for publication was Haiquan Zhao.

This method explores and analyzes the relationship between system dynamic characteristics and controller parameters. However, this method needs to alternately adjust w_c and b_0 to obtain a satisfactory dynamic performance. Wu *et al.* [21] offered an automatic adjustment algorithm for ADRC parameters, which determined the appropriate parameters by constructing a performance objective function. However, this method failed to solve the problem of effectively determining the learning interval of controller parameters. Li *et al.* [22] put forward a parameter self-tuning algorithm based on time series data mining was proposed on LADRC. Parameter tuning was performed by improving the random search algorithm of variable shrinkage coefficient, but a large amount of time series analytical data with complex computational workload were required. Liang *et al.* [23] proposed a new parameter identification method for the difficulty of tuning parameter b_0 in LADRC; but this method did not solve the tuning of other parameters in the controller. Humaidi *et al.* [24] offered a particle swarm optimization method (PSO) to tune the parameters of LADRC. The results indicated that the proposed algorithm had minimum error variance such to enhance the dynamic performance. However, the dynamic performance of the controlled object still had a large overshoot. Wei *et al.* [25] proposed a time-varying ADRC method to adjust its parameters, but this method did not realize the active adjustment of parameters to obtain a satisfactory dynamic performance. Chen *et al.* [26] proposed an adaptive method of ADRC parameters based on Q-learning. The result showed the proposed algorithm had the advantages of robustness and higher tracking precision. But there is no performance indicator to evaluate the result. Liu *et al.* [27] proposed an adaptive linear active disturbance rejection control (LADRC) controller to reduce the difficulty of parameter tuning. the number of tuning parameters of LADRC was also reduced to two by a pole placement design. However, the remaining parameter tuning task of ALADRC was still very arduous. Li *et al.* [28] investigated a method for the stable area of LADRC controller parameters and introduced a genetic algorithm to optimize controller parameters and obtain acceptable results. However, this method fails to solve and determine the upper limit of position maps. These studies demonstrate the importance of parameter optimization in LADRC. Cui *et al.* [29] proposed a specific parameter tuning formula for second-order linear active disturbance rejection controller (LADRC).The results could achieve satisfactory performance in disturbance rejection and robustness. But the dynamic performance of the rise time was too long. Liu *et al.* [30] proposed a measurement delay compensated linear ADRC (LADRC), and a simple tuning method for LADRC's parameters was presented. However, it was based on an ideal model without resistance.

Hence, we adopt the idea of error elimination based on error. The combination of adaptive algorithm and LADRC realizes online adaptive optimization of parameters in its controller. The rest of this paper is organized as follows. The nonlinear mathematical model of the magnetic levitation ball system is established in Section 2. The proposed algorithm is designed, derived, and proven in Section 3. The simulation and experimental results are discussed in Section 4. Finally, conclusions and direction of future work are presented in Section 5.

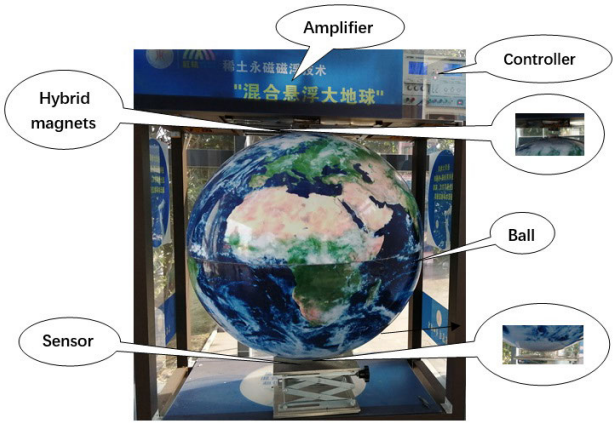

FIGURE 1. A magnetic levitation ball system.

II. NONLINEAR MODEL OF MAGNETIC LEVITATION BALL SYSTEM

A. SYSTEM INTRODUCTION

The magnetic levitation ball system is shown in Fig. 1.The magnetic levitation ball control system, an experimental platform for investigating the magnetic levitation technology, consists of a hybrid magnet, a laser sensor, a ball, and a power amplifier. The hybrid magnet is realized by installing a permanent magnet in the middle of a U-shaped electromagnet. The system also includes a laser sensor that determines the position of the magnetic ball relative to the coil.

The system uses a hybrid magnet to achieve the suspension of the magnetic ball at the equilibrium position with the following principles: First, the laser sensor detects and determines the position signal of the magnetic ball in real time. The control signal is used as the input signal of the controller and calculated via the control algorithm to output the control signal. Second, the control signal is transformed into the control current through the power amplifier. Finally, the control current is used to drive the generation of magnetic force in the hybrid magnet to resist the magnetic ball. Meanwhile, the magnetic ball is constantly maintained at a balanced position due to gravity.

Fig.2 exhibits the structure of magnetic levitation ball control system. The suspension height is the distance from the magnetic ball to the surface of the hybrid magnet. The magnetic levitation ball system has nonlinear characteristics. And it has been theoretically verified in the mathematical modeling process of the system. The magnetic levitation ball system is an open-loop unstable system. Given that a nonlinear relationship between the hybrid magnetic force and the levitation height, this balance is extremely unstable. The magnetic suspension ball falls when external disturbance (such as voltage fluctuations or wind) occurs. Thus, a closed-loop control system must be used.

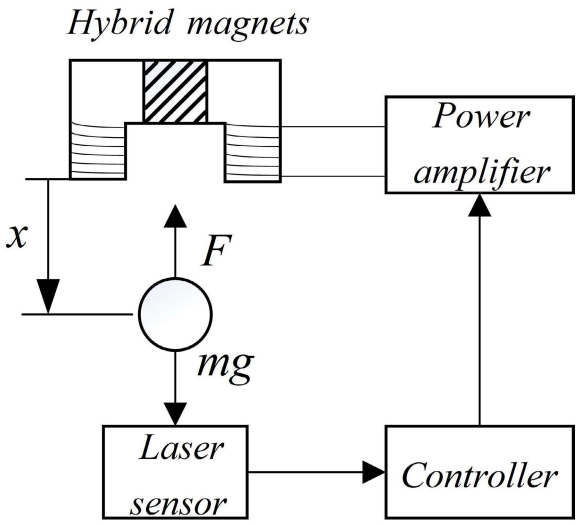

FIGURE 2. Structure of magnetic levitation ball system.

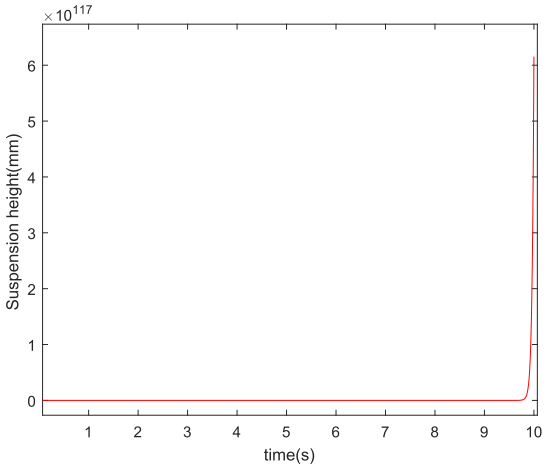

FIGURE 3. The position response of magnetic levitation ball open loop system.

B. MODEL OF MAGNETIC LEVITATION BALL SYSTEM

By analyzing the structure and principle of the magnetic levitation ball mentioned-above, a mathematical model based on the permanent magnet and electromagnetic hybrid magnetic levitation ball was established. According to Newton's second and Kirchhoff's laws, the dynamics of the magnetic ball in the vertical direction can be expressed as follows:

$$m\frac{d^2x}{dt^2} = F(x,i) - mg + f_d \tag{1}$$

$$u = Ri + \frac{\mu_0 N^2 s}{(2x + H_c h_{mp})}\frac{di}{dt} - \frac{2\mu_0 Ns(Ni + H_c h_{mp})}{(2x + H_c h_{mp})^2}\frac{dx}{dt} \tag{2}$$

$$F(x,i) = \frac{B^2 s}{\mu_0} = \mu_0 s\left(\frac{Ni + H_c h_{mp}}{2x + h_{mp}/\mu_r}\right)^2 \tag{3}$$

The formula(1) describes the dynamics of magnetic levitation ball, where f_d is the external interference force. Compared with the levitation force provided by pure electromagnetics, the hybrid magnetic force is more complicated. It is also provided by a mixture of permanent magnets and electromagnets in the formula(3).The presence of hybrid magnetic force, which is nonlinear with the current and distance as well as the square of the ratio of current and distance, changes the relationship among the distance, current, and magnetic force due to the addition of permanent magnets. The material and the length of permanent magnets affect this force.

If the magnetic ball is in a balanced position, then its gravity and hybrid magnetic force are equal. The point (x_0, i_0) is the stable equilibrium point of the magnetic levitation ball system. In this task, it is necessary to achieve the linearization of magnetic force at this equilibrium point. Thereafter, the hybrid magnetic force with the Taylor series is then expanded at the equilibrium position of the magnetic levitation ball system while ignoring the higher-order terms. Thus, the hybrid magnetic force $F(x, i)$ can be expressed as follows:

$$F(x,i) = F(x_0,i_0) + k_i(i - i_0) + k_x(x - x_0) \tag{4}$$

We define k_i and k_x to facilitate the subsequent design:

$$k_i = \left.\frac{\partial F}{\partial i}\right|_{(x_0,i_0)} = \frac{2\mu_0 Ns(Ni_0 + H_c h_{mp})}{(2x_0 + h_{mp}/\mu_r)^2}$$

$$k_x = \left.\frac{\partial F}{\partial x}\right|_{(x_0,i_0)} = -\frac{4\mu_0 Ns(Ni_0 + H_c h_{mp})^2}{(2x_0 + h_{mp}/\mu_r)^3}$$

The above-mentioned formulas can be simplified, and the following formula can be obtained:

$$m\ddot{x} = k_x x - k_i i + f_d \tag{5}$$

The magnetic levitation ball system model takes current i as input and levitation height x as output. We assign the state variable $x_1 = y, x_2 = \dot{y}, x_3 = f$. Accordingly, the magnetic levitation ball system can be expressed as follows:

$$\begin{cases} \dot{x} = Ax + Bu + E\dot{f} \\ y = Cx \end{cases} \tag{6}$$

where

$$A = \begin{bmatrix} 0 & 1 & 0 \\ 0 & 0 & 1 \\ 0 & 0 & 0 \end{bmatrix}, B = \begin{bmatrix} 0 \\ b_0 \\ 0 \end{bmatrix}, E = \begin{bmatrix} 0 \\ 0 \\ 1 \end{bmatrix}, C = \begin{bmatrix} 1 & 0 & 0 \end{bmatrix}$$

f is variable, and it represents the total interference, which includes the sum of internal and external interference.

The following assumptions are made before the magnetic levitation ball system modeling:

(1) Ignore the magnetic resistance of the iron core;

(2) Ignore factors, such as magnetic leakage and remanence;

(3) The magnetic flux in the hybrid magnet is evenly distributed.

Actual model parameter values and physical meanings of the magnetic levitation ball system are listed in Table 1.

TABLE 1. Parameters of the magnetic levitation ball system.

Variable and Descriptions	Values
The mass of magnetic ball $m(kg)$	2
Coil turns N	5000
Current in the coil at balance $i_0(A)$	1.18
The suspension height when the magnetic ball is balanced $x_0(m)$	0.01
Magnetic pole area $s(m^2)$	$3.644\pi \times 10^{-4}$
Permeability of vacuum $\mu_0(H/m)$	$4\pi \times 10^{-7}$
Relative permeability μ_r	1
The length of the permanent magnet $h_{mp}(m)$	0.03
The coercive force of permanent magnet $H_c(kA/m)$	800
Coil resistance $R(\Omega)$	13.6

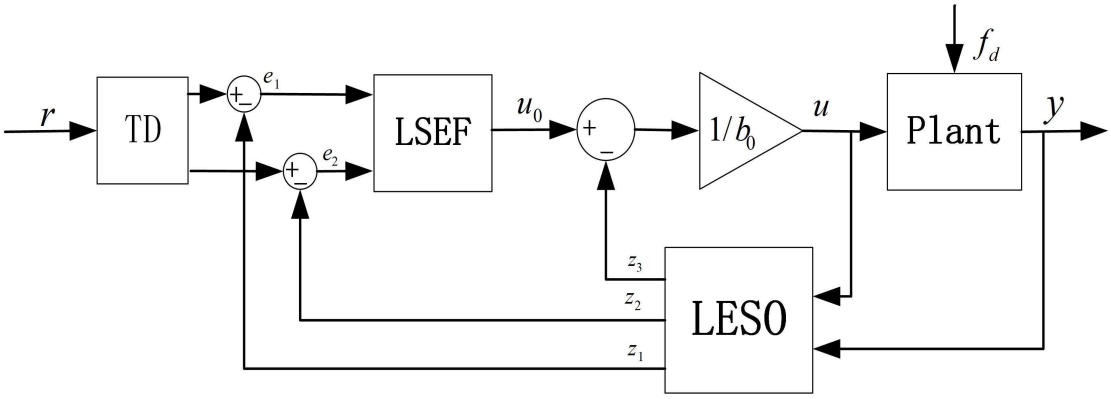

FIGURE 4. The structure of LADRC.

Fig.3 can be obtained by substituting the previous parameter values into the magnetic levitation ball system. The curve demonstrates that the magnetic levitation ball system is divergent. This fact proves the instability of the magnetic levitation ball system once again. Therefore, a closed-loop control system must be used to achieve the stable suspension of the magnetic levitation ball.

III. PARAMETER TUNING OF MAGNETIC LEVITATION BALL SYSTEM

A. STRUCTURE OF LADRC

The wide range of applications of LADRC is due to its strong anti-interference capabilities, which are also independent of the model of the controlled object. The structure of LADRC is illustrated in Fig.4. It is composed of three parts, namely, the Tracking Differentiator (TD), the Linear Extended State Observer (LESO), and the Linear State Error Feedback (LSEF).

TD is used to arrange the transition process of the control system, it also generates the signal input by the controller system. LESO is the core part of LADRC, and its function is to accurately estimate the system state, error changes, and external interference. LESO is mainly used to solve the core problem of interference observation in active anti-interference technology. Moreover, LESO does not rely on the model that generates the interference, nor does it require direct measurement to observe the interference. LSEF is the input of the LADRC calculated on the basis of the output of TD and LESO.

Three parameters, namely, controller bandwidth w_c, observer bandwidth w_o and b_0,which are adjusted to obtain a satisfactory dynamic performance in LADRC. The controller bandwidth w_c determines the response speed of the system. The observer bandwidth w_o determines the tracking speed of LESO. b_0 is determined by the controlled system.

The mathematical structure of LESO can be described as follows:

$$e(t) = z_1(t) - y(t) \tag{7}$$

$$z_1(t+h) = z_1(t) + h(z_2(t) - \beta_1 e(t)) \tag{8}$$

$$z_2(t+h) = z_2(t) + h(z_3(t) - \beta_2 e(t) + b_0 u) \tag{9}$$

$$z_3(t+h) = z_3(t) + h(-\beta_3 e(t)) \tag{10}$$

As shown in Fig. 4, we can know that y is the magnetic levitation ball system output, it stands for suspension height. u is control system input. β_1,β_2 and β_3 are tunable gains of LESO, and they have a certain relationship with w_c,which defined as: $\beta_1 = 3w_c$, $\beta_2 = 3{w_c}^2$, $\beta_3 = {w_c}^3$. z_1 represents the suspension height value observed by the state observer in LESO. z_2 is the derivative of z_1,and it also means the speed of the magnetic ball.z_3 is the total interference of the system, which includes the sum of internal and external interferences. h is denoted as the sampling step.

The second element of LADRC is LSEF, which can be represented by the following sets of formulas:

$$e_1(t) = y_r(t) - z_1(t) \tag{11}$$

$$e_2(t) = -z_2(t) \tag{12}$$

$$u_0 = k_p e_1 + k_d e_2 \tag{13}$$

$$u = \frac{u_0 - z_3}{b_0} \tag{14}$$

where y_r is the setting suspension height value. e_1 and e_2 stand for the error sum between the input signals and the estimates of the state observer output. We use $e_2(t) = -z_2(t)$ instead of $e_2(t) = \dot{y}_r(t) - z_2(t)$ in formula (12) to avoid the differentiation of the set value, which also prevents the magnetic levitation ball system problems caused by the rapid change of the set value. k_p and k_d are the proportional and differential magnification factors, respectively, they have a certain relationship with w_c.These factors can be defined as: $k_p = w_c^2$, $k_d = 2w_c$.

b_0 is a tunable parameter in the magnetic levitation ball system. Formula (13) is the generation of control signals; thus, it can greatly eliminate the influence of external interference. Formula (14) is the control variable generated by reducing total interference.

B. DESIGN OF A-LADRC

In LADRC, manual parameter adjustment is used to obtain the satisfactory dynamic performance of the system, and its process is complicated. This study mainly combines adaptive algorithms and LADRC to realize parameter optimization in its controller. This method is called adaptive linear active disturbance rejection control(A-LADRC).

First, the following formula is set to perform the adaptive tuning of parameter w_o in LADRC:

$$w_o(t) = e^{\lambda(t+h)} \tag{15}$$

where $e_{11}(t) = z_1(t+h) - y(t)$, $e_{22}(t) = z_1(t+h) - r(t)$. Thus, the weight update of $\lambda(t+h)$ can be obtained by using the following formula:

$$\lambda(t+h) = \lambda(t) + 2\alpha \frac{1}{(3hw_o - 1)} \frac{e_{22}}{(e_{11} + \varepsilon)} \tag{16}$$

where α is the regulatory factor, which can also be considered as a positive number.$\lambda(t)$ is the initial value of w_c. h is a sampling step and we set it to 0.001. ε is the allowable error value between the estimated value of the state variable in LESO and the actual output value. The existence of ε can improve the simulation effect, and its value is close to zero.

Finally, we use Lyapunov to prove the convergence of the adaptive algorithm. This expression chooses the following Lyapunov function.

$$V = \frac{1}{2}({e_{11}}^2 + {e_{22}}^2) \tag{17}$$

The result shows that:

$$V > 0$$

where $\dot{V}$ is the derivative of V, next we prove the positive or negative of $\dot{V}$. Thus the equation of $\dot{V}$ can be obtained as follows:

$$\begin{aligned}
\dot{V} &= e_{11}\dot{e_{11}} + e_{22}\dot{e_{22}} \\
&= e_{11}\frac{\partial e_{11}}{\partial t} + e_{22}\frac{\partial e_{22}}{\partial t} \\
&= e_{11}\frac{\partial\,[z_1(t+h) - y(t)]}{\partial z_1(t+h)}\frac{\partial z_1(t+h)}{\partial w_o(t)}\frac{\partial w_o(t)}{\partial \lambda(t+h)}\frac{\partial \lambda(t+h)}{\partial t} \\
&\quad + e_{22}\frac{\partial\,[z_1(t+h) - r(t)]}{\partial z_1(t+h)}\frac{\partial z_1(t+h)}{\partial w_o(t)}\frac{\partial w_o(t)}{\partial \lambda(t+h)}\frac{\partial \lambda(t+h)}{\partial t} \\
&= e_{11}(1\text{-}\frac{1}{3hw_o})(\text{-}3he)(w_o)(2\alpha\frac{1}{h(3hw_o - 1)}\frac{e_{22}}{e_{11} + \varepsilon}) \\
&\quad + e_{22}(\text{-}3he)(w_o)(2\alpha\frac{1}{h(3hw_o - 1)}\frac{e_{22}}{e_{11} + \varepsilon}) \\
&= -\frac{2\alpha e e_{22}}{h(e_{11} + \varepsilon)}e_{11} - \frac{3hw_o}{3hw_o - 1}\frac{2\alpha e e_{22}}{h(e_{11} + \varepsilon)}e_{22} \\
&< -\frac{2\alpha e e_{22}}{h(e_{11} + \varepsilon)}e_{11} - \frac{2\alpha e e_{22}}{h(e_{11} + \varepsilon)}e_{22} \\
&< \frac{-2\alpha e_{11}e_{22}}{h} - \frac{2\alpha {e_{22}}^2}{h} < \frac{-4\alpha {e_{22}}^2}{h} < 0
\end{aligned}$$

The following equation is transported to prove $\dot{V}$:

$$\lim_{t\to\infty} z_1(t+h) = z_1(t) \tag{18}$$

The boundedness and convergence of the magnetic levitation ball system are proved. The parameter optimization of w_0 becomes the relationship between λ and α in the weight update formula. Based on multiple experimental data, the initial value ranges from three to four, thus it reduces the influence of the initial value in the weight update formula. The relationship between the initial value and the regulatory factor can be obtained through multiple experiments.

$$\lambda(t) = 1.34\alpha^2 - 2.59\alpha + 4.28 \tag{19}$$

We use the previous method to tune the parameter w_c adaptively. The following formula is set:

$$w_c(t) = e^{\eta(t+h)} \tag{20}$$

where $e_1(t) = r(t) - z_1(t+h)$, and $e_2(t) = -z_2(t)$. Thus, the weight update of $\eta(t+h)$ can be obtained by the following formula:

$$\eta(t+h) = \eta(t) + 2\mu\frac{1}{(w_c e_1 + e_2)}\frac{e_1}{(e_2 + \varepsilon)} \tag{21}$$

where μ is the regulatory factor and also a positive number. $\eta(t)$ is the initial value of w_c.We use Lyapunov function to prove the convergence of the proposed algorithm as follows:

$$V = \frac{1}{2}(e_1{}^2 + e_2{}^2) \tag{22}$$

Accordingly, the following expression can be easily obtained:

$$V > 0$$

We calculate $\dot{V}$ and determine whether it has a positive or negative value. Thus, the $\dot{V}$ can be obtained as follows:

$$\begin{aligned}
\dot{V} &= e_1\dot{e_1} + e_2\dot{e_2} \\
&= e_1\frac{\partial e_1}{\partial t} + e_2\frac{\partial e_2}{\partial t} \\
&= e_1\frac{\partial\left[r(t) - z_1(t+h)\right]}{\partial u_0(t)}\frac{\partial u_0(t)}{\partial w_c(t)}\frac{\partial w_c(t)}{\partial \eta(t+h)}\frac{\partial \eta(t+h)}{\partial t} \\
&\quad + e_2\frac{\partial\left[-z_2(t)\right]}{\partial u_0(t)}\frac{\partial u_0(t)}{\partial w_c(t)}\frac{\partial w_c(t)}{\partial \eta(t+h)}\frac{\partial \eta(t+h)}{\partial t} \\
&= e_1(-h^2)(2w_ce_1 + 2e_2)(w_c)(2\mu\frac{1}{h(w_ce_1+e_2)}\frac{e_1}{e_2+\varepsilon}) \\
&\quad + e_2(-\frac{1}{\beta_2})(2w_ce_1 + 2e_2)(w_c)(2\mu\frac{1}{h(w_ce_1+e_2)}\frac{e_1}{e_2+\varepsilon}) \\
&= -\frac{4\mu w_c(h^2e_1{}^2 + \frac{1}{\beta_2}e_1e_2)}{h(e_2+\varepsilon)} < -\frac{4\mu w_c(\frac{1}{\beta_2}e_1e_2)}{h(e_2+\varepsilon)} \\
&< -4\mu w_c\frac{1}{h\beta_2}e_1 < 0
\end{aligned}$$

The result showed that $\dot{V}$ is less than zero; hence, the Lyapunov function has proven the convergence of the proposed algorithm. The experiments indicated that the regulatory factor μ value ranges from 0 to 0.5, and the value of initial η ranges from 3 to 3.5. The relationship between these factors can be expressed as follows:

$$\eta(t) = -1.33\mu + 3.66 \tag{23}$$

Therefore, the optimization of parameter w_o in the LESO and parameter w_c in the LSEF have been accomplished through the design, derivation, and verification of the above algorithm.

IV. SIMULINK RESULTS

We compare the proposed algorithm with A-LADRC to illustrate its superiority further by introducing the sliding mode control (SMC). The MATLAB platform is utilized to carry out the numerical simulation of parameter optimization of A-LADRC and confirm the effect on the basis of A-LADRC.

We examine the effect of SMC,LADRC and A-LADRC on their anti-interference ability according to the three error criteria. The three error criteria are integral of absolute-value of error (IAE), integral of time-multiplied absolute-value of error (ITAE), and integral of time multiplied by squared error (ITSE). These criteria can be expressed by the following formulas:

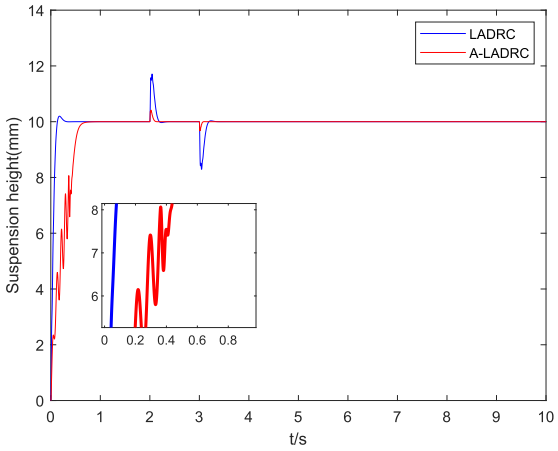

(a)

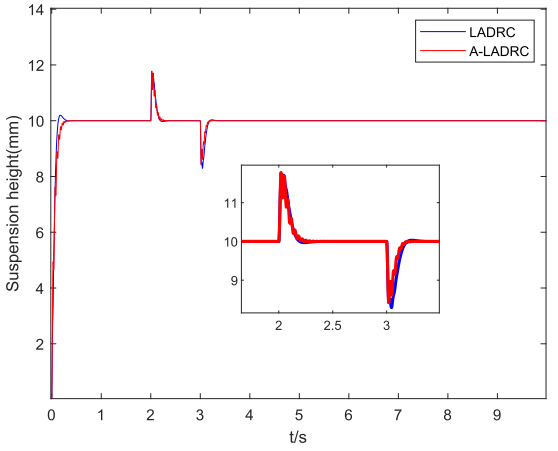

(b)

FIGURE 5. Influence of initial value on A-LADRC.

$$IAE = \int_0^t |e_y|d\tau = \int_0^t |y_r - y_{out}|d\tau \tag{24}$$

$$ITAE = \int_0^t t\,|e_y|d\tau = \int_0^t t\,|y_r - y_{out}|d\tau \tag{25}$$

$$ITSE = \int_0^t |e_y|^2\,d\tau = \int_0^t (y_r - y_{out})^2\,d\tau \tag{26}$$

where y_r is the set suspension height value, and the y_{out} is the suspension height value output by the magnetic levitation ball system.

However, the regulatory factor and initial value in the adaptive algorithm must be determined before conducting the following experiments(case studies),because they can remarkably affect the result.

Chattering phenomenon is caused by the small initial value as shown in Fig.5(a); when the regulatory factor gets larger, the anti-interference ability drops again as shown in Fig.5(b). This finding also demonstrated that the selection of initial values is crucial in A-LADRC.

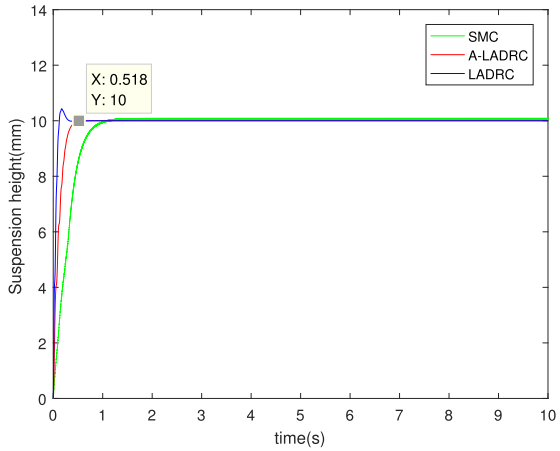

(a)

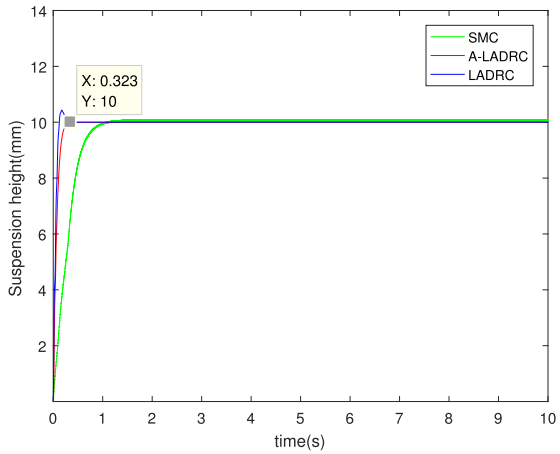

(b)

FIGURE 6. The effect of A-LADRC under different regulatory factors.

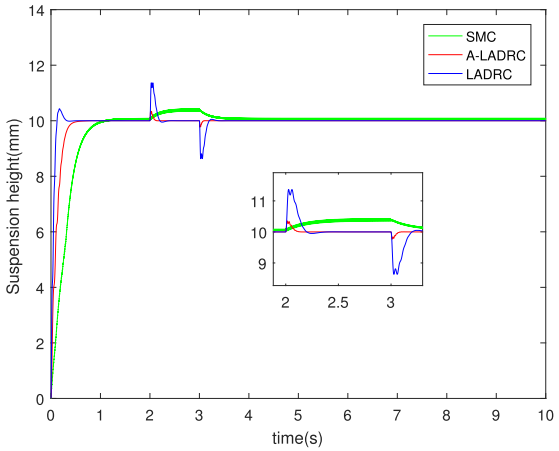

(a)

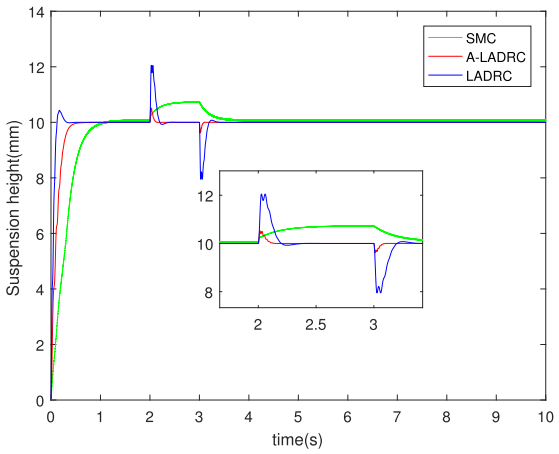

(b)

FIGURE 7. Anti-interference ability under different interferences.

The following experiments are presented in four cases. The step signal is initially taken as the reference signal. The performance of the anti-interference ability of SMC, LADRC, and A-LADRC are then compared. Finally, sinusoidal and square wave signals are alternately used as the reference signal to compare the tracking effect and anti-interference ability of SMC, LADRC, and A-LADRC.

1) CASE 1

The step signal is input as the reference signal to verify the effect of A-LADRC. Adaptive parameters α and μ are set to 0.1 in Fig.6(a). The values of α and μ are set at 0.2 in Fig.6(b). The initial values of λ and η remain unchanged. It can be seen that the SMC can achieve the stable suspension of the magnetic levitation ball from Fig.6 (a) and (b), but its rise time is excessively long. Although the rise time of LADRC is too short, it has a large overshoot. Only A-LADRC satisfies their shortcomings. An appropriate increase in the regulatory factor can reduce its rise time. We can see that the rise time of A-LADRC is 0.518 s to 0.323 s from Fig.6(a) and (b), and the rise time has been reduced by 37.64%.The overshoot of A-LADRC is significantly smaller than LADRC. Hence, A-LADRC demonstrates better dynamic performance than SMC and LADRC.

2) CASE 2

The robustness and anti-interference ability of SMC, A-LADRC, and LADRC under different interferences are investigated in this case. The interference is set to 20 and 40 N to determine their effects at 2 s. We can obtain the experimental results and data using the three error criteria and their anti-interference ability is illustrated Figs. 7(a) and 7(b).

The suspension height of LADRC changes by approximately 2 mm when the interference varies from 20 N to 40 N. SMC changes by approximately 0.5 mm with an excessively long duration. Only the suspension height of A-LADRC is basically the same as that of A-LADRC at 20 N. This finding reflects their anti-interference ability.

Table 2 presents the twofold improvement of the three error criteria of SMC. However, the error of ITAE improved by only 29.75% in A-LADRC. By comparison, the error of ITAE increased by 52.53% in LADRC. Therefore, A-LADRC

TABLE 2. Comparisons of three error criterions under different interferences.

Reference signal	Controller	IAE	ITAE	ITSE
Step+interference(20N)	SMC	3.874×10^{-3}	5.445×10^{-3}	3.134×10^{-6}
	LADRC	7.611×10^{-4}	7.251×10^{-4}	7.572×10^{-7}
	A-LADRC	7.217×10^{-4}	1.348×10^{-4}	2.001×10^{-7}
Step+interference(40N)	SMC	6.467×10^{-3}	1.239×10^{-2}	2.342×10^{-5}
	LADRC	9.010×10^{-4}	1.106×10^{-3}	1.629×10^{-6}
	A-LADRC	8.655×10^{-4}	1.749×10^{-4}	2.209×10^{-7}

TABLE 3. Comparisons of three error criterions under sinusoidal signal.

Reference signal	Controller	IAE	ITAE	ITSE
Sinusoidal	SMC	4.744×10^{-3}	1.565×10^{-2}	7.275×10^{-6}
	LADRC	2.674×10^{-3}	1.135×10^{-2}	3.256×10^{-6}
	A-LADRC	2.304×10^{-3}	7.995×10^{-3}	1.875×10^{-6}
Sinusoidal+interference	SMC	5.334×10^{-3}	1.741×10^{-2}	9.637×10^{-6}
	LADRC	2.901×10^{-3}	1.250×10^{-2}	3.967×10^{-6}
	A-LADRC	2.702×10^{-3}	7.302×10^{-3}	1.640×10^{-6}

adopts self-adaptive real-time parameter optimization and its three errors are significantly less than those of SMC and LADRC. This finding proves the strong robustness and anti-interference ability of A-LADRC.

We also performed additional experimental tests under different interferences in the range of 0–50 N to illustrate the robustness of A-LADRC further. Notably, the total interference of LADRC includes the sum of internal and external interferences. The total interference of the magnetic ball system is estimated and compensated through the LESO in this study.

From Fig. 8 (a), (b) and (c), we can get the following conclusions: the three errors of A-LADRC are far smaller than LADRC when the interference changes continuously within a certain range regardless of the error criterion used in IAE, ITAE, and ITSE. Because A-LADRC adopts adaptive algorithm for real-time adaptation parameter optimization. This phenomenon is clearly reflected with the increase of interference. The results proved the superiority of A-LADRC by demonstrating that the strong anti-interference ability of A-LADRC self-adjusts under self-adaptation.

3) CASE 3

The sinusoidal signal is input as the reference signal in this case to analyse the tracking effect of SMC, A-LADRC, and LADRC when their suspension heights change in a sine function. Both α and μ are set to 0.1.The initial value of λ is 4, and the initial value of η is 3.5.The amplitude of the sinusoidal signal is 3, and the frequency is 3 Hz. Thus, the sinusoidal signal can be expressed as follows:

$$y_r = 10 + 3\sin(3t) \tag{27}$$

The reference signal is to change the suspension height value in the range of 7-13 mm with the sinusoidal signal. We can see the tracking effect of SMC,A-LADRC, and LADRC without interference are illustrated in Fig.9(a). A step interference signal of 5 N is added as the interference signal. The tracking effect of A-LADRC under interference is shown in Fig. 9(b).

Table 3 presents the experiment data of the sinusoidal signal under the three error criteria with or without interference. The error of IAE in A-LADRC is smaller than LADRC and SMC. The two error indicators of ITAE and ITSE are also both smaller than those without interference in A-LADRC. ITAE and ITSE errors reduce by 8.66% and 12.53%, respectively. However, the error of LADRC becomes significantly larger after adding the interference. Respective errors of ITAE and ITSE improve by 10.13% and increase by 21.84% in LADRC.

We can get the following conclusion from the Fig.9 (a), (b) and Table 3: when a sinusoidal signal is input as the reference signal with or without interference, A-LADRC can achieve its perfect tracking, then LADRC, and finally it's SMC. Hence, this finding proves the superiority and novelty of A-LADRC.

4) CASE 4

Tracking effects of SMC, A-LADRC, and LADRC when suspension heights change and the square wave signal is input

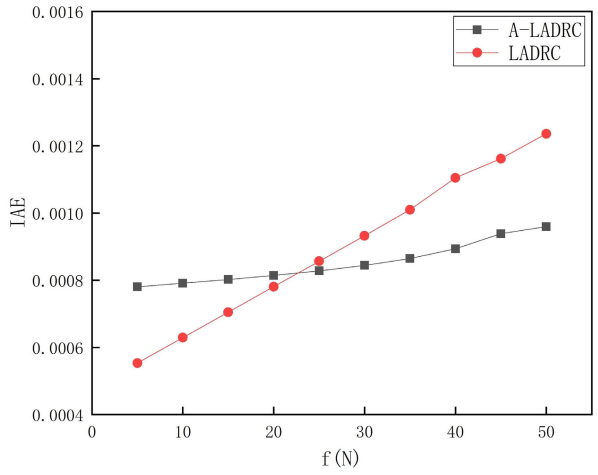

(a)

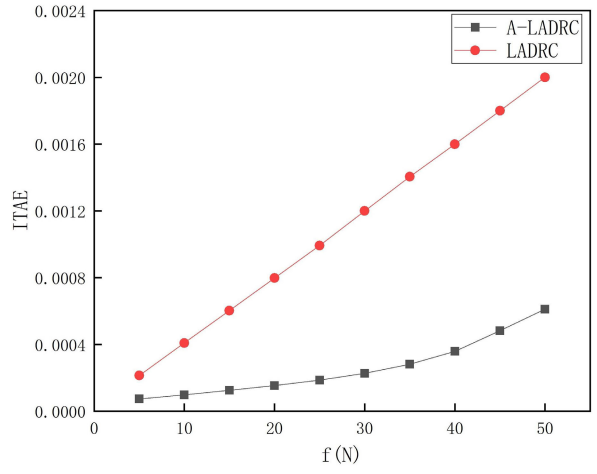

(b)

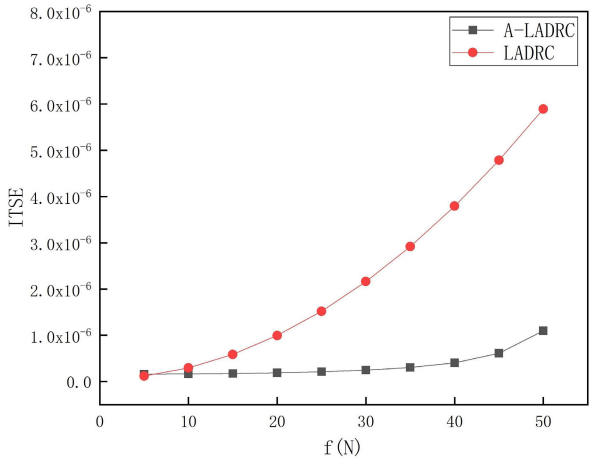

(c)

FIGURE 8. Comparison of errors between A-LADRC and LADRC under interference changes.

as the reference signal are compared. The adaptive parameter value in A-LADRC is the same as the previous sinusoidal signal parameter value. The period of square wave signal is

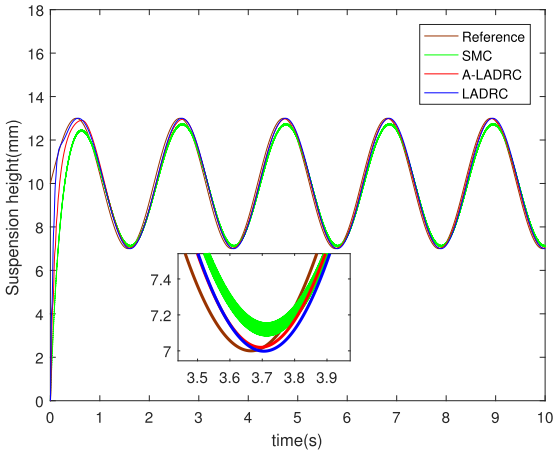

(a)

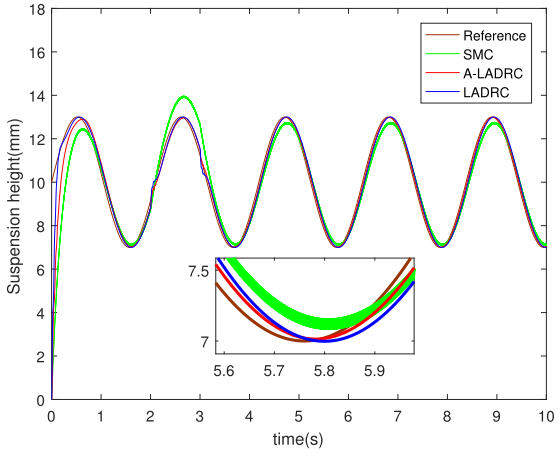

(b)

FIGURE 9. Tracking effect of A-LADRC under sinusoidal signal.

set to 2, and the duty ratio is 50%.Thus, the square wave signal can also be expressed as follows:

$$y_r = \begin{cases} 12mm & k \le t \le k+1 (k = 0, 2, 6 \ldots\ldots) \\ 10mm & k \le t \le k+1 (k = 1, 3, 5 \ldots\ldots) \end{cases} \tag{28}$$

Tracking effects of SMC, LADRC, and A-LADRC are illustrated in Fig. 10(a). In addition, an interference force of 5 N is added to compare their anti-interference ability. The effect is shown in Fig. 10(b). Table 4 presents the error of the square wave signal under the three error criteria with or without interference.

When the interference is added to the square wave signal, it can be found that the three error criteria are obviously larger from the data of Table 4, it's the same as the sinusoidal signal. The error of IAE under A-LADRC is smaller than SMC and LADRC with or without interference. The error of ITAE has dropped by 23.43% in A-LADRC, the error of ITSE is also reduced by 34.72% too. By comparison, the error of ITAE improved by 2.77% and that of ITSE increased by 5.77% in LADRC. Hence, A-LADRC can successfully approximate

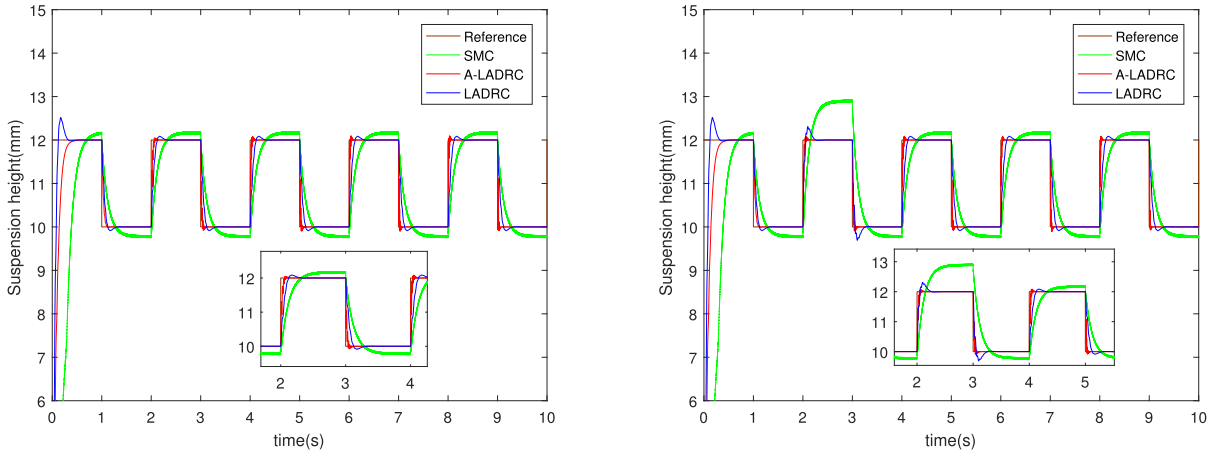

FIGURE 10. Tracking effect of A-LADRC under square wave signal.

TABLE 4. Comparisons of three error criterions under square wave signal.

Reference signal	Controller	IAE	ITAE	ITSE
Square	SMC	5.651×10^{-3}	1.592×10^{-2}	1.460×10^{-5}
	LADRC	1.372×10^{-3}	4.283×10^{-3}	4.512×10^{-6}
	A-LADRC	1.080×10^{-3}	1.127×10^{-3}	1.439×10^{-6}
Square+interference	SMC	6.619×10^{-3}	1.855×10^{-2}	1.901×10^{-5}
	LADRC	1.444×10^{-3}	4.402×10^{-3}	4.746×10^{-6}
	A-LADRC	1.158×10^{-3}	8.629×10^{-4}	9.394×10^{-7}

the square wave signal while adopting adaptive parameters with or without interference in the optimization.

Therefore, the tracking effect of A-LADRC is significantly better than that of SMC and LADRC with or without interference when sinusoidal and square wave signals are inputted as reference signals. This finding is clearly illustrated by the three error criteria (IAE, ITAE, and ITSE) introduced in the evaluation. Experimental data listed in Tables 2, 3, and 4 demonstrated that the error of A-LADRC is significantly smaller than that of SMC and LADRC regardless of the error criterion used. This finding further proves the novelty and superiority of A-LADRC.

V. CONCLUSION

In this study, the LADRC is mainly used to achieve the stable suspension of the magnetic ball. The adaptive algorithm is combined with LADRC to address the difficulty of tuning controller and observer bandwidths in LADRC. This approach can realize the real-time online adaptive optimization and tuning of parameters in the controller. Effects of SMC, LADRC, and A-LADRC controllers are evaluated using their tracking performance and anti-interference ability.

The results show that only A-LADRC satisfies their shortcomings when the step signal is input as the reference signal. Compared to a fixed bandwidth LADRC, although the adaptive algorithm complexity is slightly increased, it ensures good dynamic performance and improves the anti-interference ability. The experimental data also showed that the situation is the opposite in the proposed algorithm. The three error values are smaller than those without interference. Cases 2, 3, and 4 obtained similar results. In addition, A-LADRC exhibits stronger anti-interference ability than SMC and LADRC due to its adoption of adaptive real-time parameter optimization. The effect intensifies with the increase of interference. The tracking effect of A-LADRC is significantly higher than that of SMC and LADRC with or without interference when sine and square wave signals are alternately input as reference signals.

If the relationship between the initial value and the regulatory factor in the proposed algorithm can be deduced and proved rather than obtained from the empirical formula, then the performance of A-LADRC will be superior in the future.

REFERENCES

[1] H. S. Han and D. S. Kim, *Magnetic Levitation*. Amsterdam, The Netherlands: Springer, 2016.
[2] H.-W. Lee, K.-C. Kim, and J. Lee, "Review of maglev train technologies," *IEEE Trans. Magn.*, vol. 42, no. 7, pp. 1917–1925, Jul. 2006.
[3] Y. Sun, W. Li, H. Qiang, and D. Chang, "An experimental study on the vibration of the low-speed maglev train moving on the guideway with sag vertical curves," *Int. J. Control Autom.*, vol. 9, no. 4, pp. 279–288, Apr. 2016.

[4] I. Boldea, L. Nicolae Tutelea, W. Xu, and M. Pucci, "Linear electric machines, drives, and MAGLEVs: An overview," *IEEE Trans. Ind. Electron.*, vol. 65, no. 9, pp. 7504–7515, Sep. 2018.
[5] H.-W. Cho, H.-S. Han, J.-S. Bang, H.-K. Sung, and B.-H. Kim, "Characteristic analysis of electrodynamic suspension device with permanent magnet Halbach array," *J. Appl. Phys.*, vol. 105, no. 7, Apr. 2009, Art. no. 07A314.
[6] L. Cheng and Z. Kun-lun, "Vertical stability analysis of permanent-magnet EDS system with permanent magnets and electromagnets hybrid Halbach array," *IFAC-PapersOnLine*, vol. 52, no. 24, pp. 65–70, 2019.
[7] Y. Sun, J. Xu, H. Qiang, C. Chen, and G. Lin, "Adaptive sliding mode control of maglev system based on RBF neural network minimum parameter learning method," *Measurement*, vol. 141, pp. 217–226, Jul. 2019.
[8] Y. Sun, J. Xu, H. Qiang, and G. Lin, "Adaptive neural-fuzzy robust position control scheme for maglev train systems with experimental verification," *IEEE Trans. Ind. Electron.*, vol. 66, no. 11, pp. 8589–8599, Nov. 2019.
[9] Y. Sun, J. Xu, G. Lin, W. Ji, and L. Wang, "RBF neural network-based supervisor control for maglev vehicles on an elastic track with network time-delay," *IEEE Trans. Ind. Informat.*, early access, Oct. 19, 2020, doi: 10.1109/TII.2020.3032235.
[10] N. Boonsatit and C. Pukdeboon, "Adaptive fast terminal sliding mode control of magnetic levitation system," *J. Control, Autom. Electr. Syst.*, vol. 27, no. 4, pp. 359–367, Aug. 2016.
[11] J. Xu, Y. Sun, D. Gao, W. Ma, S. Luo, and Q. Qian, "Dynamic modeling and adaptive sliding mode control for a maglev train system based on a magnetic flux observer," *IEEE Access*, vol. 6, pp. 31571–31579, 2018.
[12] J. de Jesus Rubio, L. Zhang, E. Lughofer, P. Cruz, A. Alsaedi, and T. Hayat, "Modeling and control with neural networks for a magnetic levitation system," *Neurocomputing*, vol. 227, pp. 113–121, Mar. 2017.
[13] J.-Q. Han, "Nonlinear design methods for control systems," *IFAC Proc. Volumes* vol. 32, no. 2, pp. 1531–1536, 1999.
[14] Q. Zheng and Z. Gao, "On practical applications of active disturbance rejection control," in *Proc. 29th Chin. Control Conf.*, Jul. 2010, pp. 6095–6100.
[15] J. Han, "From PID to active disturbance rejection control," *IEEE Trans. Ind. Electron.*, vol. 56, no. 3, pp. 900–906, Mar. 2009.
[16] Z. Gao, "Scaling and bandwidth-parameterization based controller tuning," in *Proc. Amer. Control Conf.*, Jun. 2006, pp. 4989–4996.
[17] S. Zhao and Z. Gao, "An active disturbance rejection based approach to vibration suppression in two-inertia systems," *Asian J. Control*, vol. 15, no. 2, pp. 350–362, Mar. 2013.
[18] Q. Zheng and Z. Gao, "Active disturbance rejection control: Some recent experimental and industrial case studies," *Control Theory Technol.*, vol. 16, no. 4, pp. 301–313, Nov. 2018.
[19] X. Chen, D. Li, and Z. Gao, "Tuning method for second-order active disturbance rejection control," in *Proc. 30th Chin. Control Conf.*, Jul. 2011, pp. 6322–6327.
[20] D. Yuan, X. J. Ma, Q.-H. Zeng, and X. Qiu, "Research on frequency-band characteristics and parameters configuration of linear active disturbance rejection control for second-order systems," *Control Theory Appl.*, vol. 30, no. 12, pp. 1630–1640, 2013.
[21] L. Wu, H. Bao, J. Du, and C.-S. Wang, "A learning algorithm for parameters of automatic disturbances rejection controller," *Acta Phys. Sin.*, vol. 40, no. 3, pp. 556–560, Mar. 2014.
[22] Y. Li, J. Wang, and Y. Zhang, "Self-tuning method for a linear active disturbance rejection controller," *Chin. J. Eng.*, vol. 37, no. 1, pp. 1520–1527, 2015.
[23] Q. Liang, C. Wang, and A. J. Pan, "Parameter identification of B0 and parameter tuning law in linear active disturbance rejection control," *Control Decis.*, vol. 30, no. 9, pp. 1691–1695, 2015.
[24] A. J. Humaidi, H. M. Badr, and A. H. Hameed, "PSO-based active disturbance rejection control for position control of magnetic levitation system," in *Proc. 5th Int. Conf. Control, Decis. Inf. Technol. (CoDIT)*, Apr. 2018, pp. 922–928.
[25] W. Wei, W. Xue, and D. Li, "On disturbance rejection in magnetic levitation," *Control Eng. Pract.*, vol. 82, pp. 24–35, Jan. 2019.
[26] Z. Chen, B. Qin, M. Sun, and Q. Sun, "Q-learning-based parameters adaptive algorithm for active disturbance rejection control and its application to ship course control," *Neurocomputing*, vol. 408, pp. 51–63, Sep. 2020.
[27] C. Liu, G. Luo, X. Duan, Z. Chen, Z. Zhang, and C. Qiu, "Adaptive LADRC-based disturbance rejection method for electromechanical servo system," *IEEE Trans. Ind. Appl.*, vol. 56, no. 1, pp. 876–889, Jan. 2020.
[28] D. Li, X. Chen, J. Zhang, and Q. Jin, "On parameter stability region of LADRC for time-delay analysis with a coupled tank application," *Processes*, vol. 8, no. 2, p. 223, Feb. 2020.
[29] W. Cui, W. Tan, D. Li, and Y. Wang, "Tuning of linear active disturbance rejection controllers based on step response curves," *IEEE Access*, vol. 8, pp. 180869–180882, 2020.
[30] C. Liu, G. Luo, Z. Chen, and W. Tu, "Measurement delay compensated LADRC based current controller design for PMSM drives with a simple parameter tuning method," *ISA Trans.*, vol. 101, pp. 482–492, Jun. 2020.

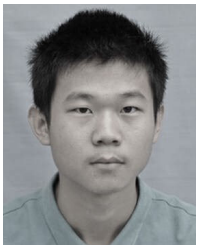

QINGHUA OUYANG (Graduate Student Member, IEEE) received the B.S. degree in automation from the Jiangxi University of Science and Technology, Ganzhou, China, in 2019, where he is currently pursuing the M.S. degree in control science and engineering. His current research interest includes magnetic levitation control.

KUANGANG FAN (Member, IEEE) was born in Linyi, China, in 1981. He received the B.S., M.S., and Ph.D. degrees in instrumentation science from Jilin University, in June 2006, June 2008, and June 2011, respectively. From 2012 to 2014, he held a postdoctoral position with the State Key Laboratory of Pattern Recognition, Institute of Automation, Chinese Academy of Sciences. From 2015 to 2016, he was a Visiting Scholar with the School of Electronics and Computer Engineering, Peking University Shenzhen Graduate School. From 2018 to 2019, he was also a Visiting Scholar with the Department of Electrical and Computer Engineering, UC Davis, Davis, CA, USA. He is currently an Associate Professor of electrical and computer engineering with the Jiangxi University of Science and Technology, China. He has published over 30 refereed articles and book chapters, and holds more than 30 invention patents. His research contributions include the broad range of signal processing and control engineering, including blind channel estimation and equalization, source separation, parameter estimation, and adaptive control.

YAHUI LIU (Student Member, IEEE) received the B.S. degree in transportation from the Anyang Institute of Technology, Anyang, China, in 2019. He is currently pursuing the M.S. degree in control engineering with the Jiangxi University of Science and Technology, Ganzhou, China. His current research interests include speed control of permanent magnetic maglev train, suspension control of permanent magnet maglev train, and speed optimization of permanent magnet maglev train.

NA LI (Student Member, IEEE) received the B.S. degree in electrical engineering and automation from the Applied Science College, Jiangxi University of Science and Technology, Ganzhou, China, in 2019, where she is currently pursuing the M.S. degree in control science and engineering. Her current research interest includes digital image processing.